Available at
www.ComputerScienceWeb.com
POWERED BY SCIENCE DIRECT®

Pattern Recognition Letters 24 (2003) 2301–2313

Pattern Recognition Letters

www.elsevier.com/locate/patrec

A lane-curve detection based on an LCF

Jong Woung Park [a,1], Joon Woong Lee [b,2], Kyung Young Jhang [c,*]

[a] Department of Precision Mechanical Engineering, Graduate School of Hanyang University, 17 Haengdang-Dong, Sungdong-Ku, Seoul 133-791, South Korea
[b] Department of Industrial Engineering, Chonnam National University, 300, Yongbong-Dong, Buk-gu, Kwangju 500-757, South Korea
[c] School of Mechanical Engineering, Hanyang University, 17 Haengdang-Dong, Sungdong-Ku, Seoul 133-791, South Korea

Received 28 August 2002; received in revised form 20 December 2002

Abstract

This paper proposes a novel image-processing algorithm to recognize the lane-curve of a structured road. The proposed algorithm uses an lane-curve function (LCF) obtained by the transformation of the defined parabolic function on the world coordinates into the image coordinates. Unlike other existing methods, this algorithm needs no transformation of the image pixels into the world coordinates. The main idea of the algorithm is to search for the best-described LCF of the lane-curve on an image. In advance, several LCFs are assumed by changing the curvature. Then, the comparison is carried out between the slope of an assumed LCF and the phase angle of the edge pixels in the lane region of interest constructed by the assumed LCF. The LCF with the minimum difference in the comparison becomes the true LCF corresponding to the lane-curve. The proposed method is proved to be efficient through experiments for the various kinds of images, providing the reliable curve direction and the valid curvature compared to the actual road.

Keywords: Lane-curve function; Image processing; Edge gradient; Lane curvature; Asymptote

1. Introduction

A lane departure warning system and a lateral control system must detect the lane in front of the vehicle. Then, the lane information is usually obtained by the computer vision, which has been the main sensing technology for lane detection. Recently, many lane detection methods have been introduced. These methods have contributed to the development of the lane departure warning and the lateral control systems. However, each of the methods has small defects, which are being solved in parts. In order to discuss the merits and demerits of the methods, we grouped methods into four types: The first type is the model-based lane (or road) detection method (Crisman and Thorpe, 1993; Kluge and Thorpe, 1992; Enkelmann et al., 1995), which has several drawbacks, such as the

* Corresponding author. Tel.: +82-2-2290-0434; fax: +82-2-2299-7207.
E-mail addresses: jongoung@ihanyang.ac.kr (J.W. Park), joonlee@chonnam.ac.kr (J.W. Lee), kyjhang@hanyang.ac.kr (K.Y. Jhang).
[1] Tel.: +82-2-2281-9206; fax: +82-2-2299-7207.
[2] Tel.: +82-62-530-1781; fax: +82-62-530-1789.

0167-8655/03/$ - see front matter
doi:10.1016/S0167-8655(03)00056-4

difficulty in detecting and matching complex road features and the complexity of the computations involved. The second type is the neural network based lane detection technology (Pomerleau, 1994; Bimbo et al., 1993; Park et al., 2001). Bimbo et al. (1993) and Park et al. (2001) detected the lane-curve by using the lane edge slope and the lane position as the input pattern of the neural network, and Pomerleau (1994) used low-resolution images as the input pattern of the neural network. The neural network based lane detection technology has the robustness to local detection errors, however it has to diversify the images to learn and needs the relearning process to detect a new lane-form, which requires a lot of processing time. The third type uses the interest region of the lane and the dynamic model of the vehicle (Behringer, 1994; Dickmanns and Mysliwetz, 1992), which make it possible to estimate the lane position easily and continuously. However, due to the local detection of the lane, it happens that noise edge features are mistaken for lane markings in bad conditions. The fourth type detects the lane-curve by means of the top-view image generation through inverse perspective mapping (Pomerleau, 1995; Bertozzi and Broggi, 1998). Pomerleau (1995) detects the lane-curve using the feature of the scan-line intensity of the top-view image and Bertozzi and Broggi (1998) uses a series of morphological filters in the top-view image. These methods showed quite good reliability, however, the top-view image must be generated during the detection process.

In this paper, a novel method using the lane-curve function (LCF) is proposed to overcome all demerits of the methods described in the above. Through the analysis of the relationship between the lane shape of the world coordinates and the lane shape of the image coordinates, we define an LCF capable of describing the lane boundary in the images. Next, the comparison of the feature of the lane image with the feature of the LCF is carried out to search for the LCF corresponding to the lane on a given image. The searched LCF is just the lane to be recognized. In this method, there are no difficulties like as in the existing methods.

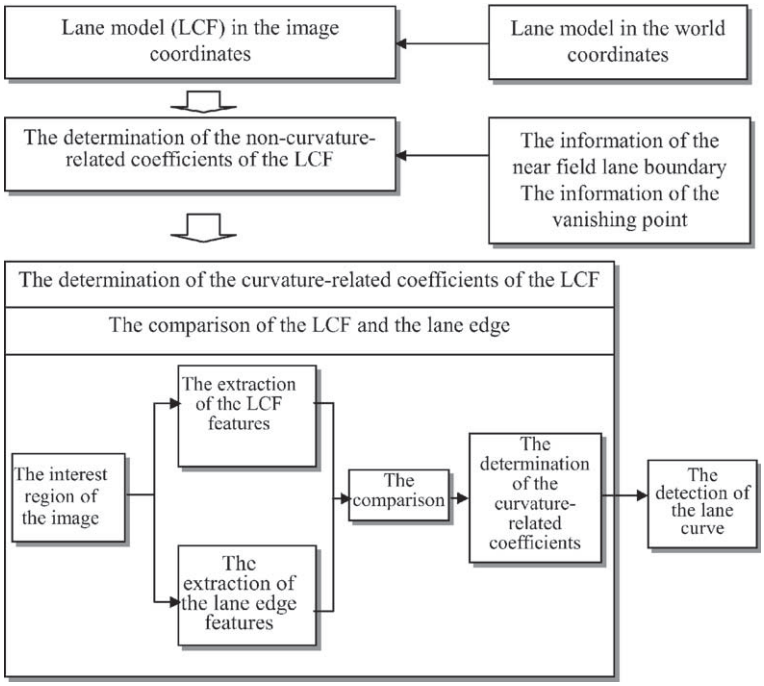

Fig. 1. Process overview.

The summarized whole process is as follows. In the first place, the proposed method premises so that the lane boundary near the camera and the vanishing point are detected. With information of these, the near lane boundary and the vanishing point, the coefficients of the LCF except for the coefficients related to the curvature are determined. Then, the unknowns are only the curvature-related coefficients. That is, if the coefficients of the LCF related to the lane-curve are extracted, the lane boundary can be perfectly described. For this, the curvature-related coefficients of the LCF are substituted for an arbitrary value in the range of the curvature limits of the superhighway, and an assumed LCF and a region of interest (ROI) around the LCF are established on a given image. If the curvature-related coefficients have the true values, the ROI will be located on the lane boundary on a given image. To find the true values of the coefficients, the edge detection is carried out in the ROI. Then, we obtain the difference between the slope of the assumed LCF and the phase angle at the edge pixel in the ROI. If the difference is small enough, the assumed LCF might be the true LCF of the lane boundary. This process is repeated until the whole values in the range of the curvature limits are considered. Fig. 1 shows the process overview.

2. Lane-curve function

2.1. World coordinate lane model and LCF

To find the model of the lane boundary in the image coordinate system, which is the LCF, the model of the lane boundary in the world coordinate system must be mathematically defined. The world coordinate lane boundary model can be approximated as a parabola (Risack et al., 2000) and expressed as follows:

$$x(y) = C + By + Ay^2/2 \tag{1}$$

When the optical axis of a camera is parallel to the lane, the direction of the lane is defined as y-axis and the perpendicular direction to the y-axis on the road surface is defined as x-axis. Then, A is a lane curvature, B is the slope of the lane boundary at origin, and C is the intersection point of the lane boundary and the x-axis. If the relationship among the world coordinate system, the camera coordinate system and the image coordinate system is established, the world coordinate lane boundary model can be transformed to the image coordinate lane boundary model as follows (see Appendix A):

$$y_f = ax_f + b + \sqrt{cx_f^2 + dx_f + e} \tag{2}$$

$$y_f = ax_f + b - \sqrt{cx_f^2 + dx_f + e} \tag{3}$$

In this paper, these two equations are called the LCF. These LCFs, (2) and (3), make a pair and depict a lane boundary. The geometric meaning of these LCFs is shown in Fig. 2. Eq. (2) corresponds to the lane boundary near to the camera, which is called the near field LCF and Eq. (3) corresponds to the lane boundary close to the vanishing line, which is called the far field LCF. The near field LCF and the far field LCF meet at the inflection point. As shown in Fig. 2, the near field LCF approaches a straight-line as it gets nearer to the near field lane boundary and the far field LCF approaches a straight-line as it gets nearer to the vanishing line. Therefore, the straight-line to which the near field LCF of Eq. (2) approaches is

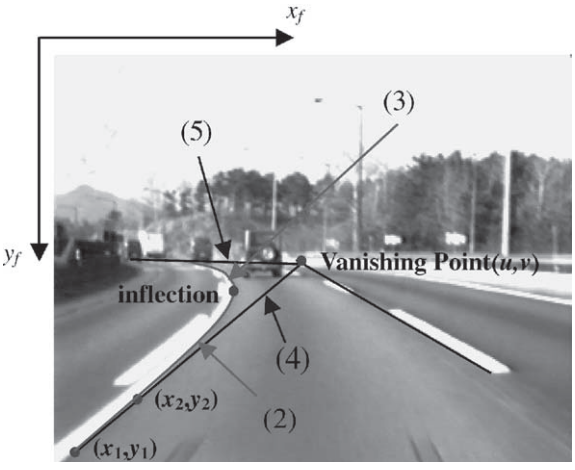

Fig. 2. LCF and its asymptotes. (2) is the near field LCF, (3) is the far field LCF, (4) is the near field asymptote, and (5) is the far field asymptote. The numbering figures are the equation numbers in this paper.

defined as the near field asymptote, and the straight-line to which the far field LCF of Eq. (3) approaches is defined as the far field asymptote. Accordingly, if the near field asymptote and the far field asymptote are computed, the non-curvature-related coefficients of the LCF can be obtained. The numerical expressions of the near field asymptote and the far field asymptote are as follows (see Appendix B):

$$y_f = (a + \sqrt{c})x_f + \left(b + c\frac{d}{2\sqrt{c}}\right) \tag{4}$$

$$y_f = (a - \sqrt{c})x_f + \left(b - \frac{d}{2\sqrt{c}}\right) \tag{5}$$

The near field LCF and the far field LCF have the five unknown coefficients, a, b, c, d, e. However, the asymptotes of Eqs. (4) and (5) have only the coefficients a, b, c, d. Therefore, it is imagined that the curvature information of the LCF is included in the coefficient e. To prove the fact that the coefficient e has the curvature information of the LCF, the relationship between the world coordinate lane model of Eq. (1) and the LCFs of Eqs. (2) and (3) was expressed mathematically in Appendix A. As expected, the curvature information A is included only in the coefficient e.

Now we assume the far field asymptote as $y = m_h + n_h$ and the near field asymptote as $y = m_n + n_n$. Then the relationship between the asymptotes of the LCF and the world coordinate lane model of Eq. (1) is expressed mathematically as follows (see Appendix C):

$$\begin{aligned} m_h &= a - \sqrt{c} = 0 \\ n_h &= b - \frac{d}{2\sqrt{c}} = C_y = v \pm \mu \\ m_n &= a + \sqrt{c} \\ n_n &= b + \frac{d}{2\sqrt{c}} \end{aligned} \tag{6}$$

where v is the value of y-axis at the vanishing point. In Eq. (6), the slope m_h of the far field asymptote is zero, which means that the road surface is flat. Also, if the optical axis of the camera is parallel to the road surface, the far field asymptote is expressed as $y = C_y$, in which C_y is the center of the y-axis of the image coordinates. Actually, the optical axis of the camera may be non-parallel to the road surface and the test vehicle may have a pitch motion. Therefore, $y = C_y \pm \mu = v$, where μ is constant for considering the fluctuation of vanishing line.

2.2. The determination of the coefficients of LCF

The determination of the unknown coefficients a, b, c, d, e of the LCF is explained in the next paragraph. By Eq. (6), the coefficients a, b, c, d are determined as follows:

$$\begin{aligned} a &= \frac{m_n}{2} \\ c &= \frac{m_n^2}{4} \\ b &= \frac{v + n_n}{2} \\ d &= \frac{m_n}{2}(n_n - v) \end{aligned} \tag{7}$$

m_n and n_n in Eq. (7) can be found in the area near the camera. In the near field area, the lane boundary can be considered a straight-line. In this paper, to find m_n and n_n, the existing method referred in the reference (Lee et al., 2001) was applied. In the existing method, the straight-line equation of the left and the right lane boundaries was found. Then, the two points, (x_1, y_1) and (x_2, y_2) as shown in Fig. 2, are selected at arbitrary points on the extracted straight-line, from which the lane slope, m_n, and the lane position, n_n, can be calculated. The vanishing point, (u, v) in Fig. 2, can be also calculated from the intersection point of the extracted straight-lines for the left and the right lane boundaries.

To determine the curvature-related coefficient e, the parameter k substitutes for the constant term including the curvature. Parameter k is set as follows:

$$e = (b - v)^2 + ka \quad (k = (-A\lambda^2 T_z)/(d_{px}d_{py})) \tag{8}$$

If the term A in Eq. (8) is zero, the parameter k becomes zero, which means that the lane is straight, and eventually the LCFs of Eqs. (2) and (3) must be straight-line equations. To make Eqs. (2) and (3) straight-line form, the quadratic equation of the inner of the square root of Eqs. (2) and

(3) must be a square. Then, e is equal to $d^2/4c$, and eventually Eqs. (2) and (3) change into Eqs. (4) and (5), respectively. Also, if k in (8) is zero, e is $(b - v^2)$. Then, the two equations $e = (b - v)^2$ and $e = d^2/4c$ will have the same expression. This relation can be derived by Eq. (7), and is as follows:

$$(b - v)^2 = \frac{d^2}{4c} = \left(\frac{n_n - v}{2}\right)^2 \tag{9}$$

In the meantime, the constants, λ, T_z, d_{px}, d_{py} in Eq. (8), have positive values, while the curvature A in Eq. (1) is positive in the right-curved lane and negative in the left-curved lane. If the signs of these constants are applied to Eq. (8), k is negative in the right-curved lane and positive in the left-curved lane, and also zero in the straight lane. If the curvature A varies from -2.192×10^{-3} (1/m) to 2.192×10^{-3} (1/m) with the step, 4.566×10^{-5} (1/m), the value of k is changed as follows:

$$k = \varepsilon i \quad (\varepsilon = 25,\ i = -48, -39, -38, \ldots, 0, 1, \ldots, 48) \tag{10}$$

Fig. 3 shows the various LCFs that are superimposed on a left-curved lane image, changing the value of i in Eq. (10) to 30, 15, 0, −15, and −30, respectively. We can know that the LCFs reflect well the curved direction of the lane boundary.

Now, it is necessary to determine the curvature index i in Eq. (10) that makes the LCF most identical to the lane on the image. The next chapter deals with the determination of the curvature index.

3. The detection of the lane-curve

3.1. Lane region of interest

Lane region of interest (LROI) is established around the LCF constructed on a given image by the method explained in the previous chapters. The LROI is the area between the value of y of the vanishing point and a heuristically determined upper point of the near field area in which the lane can be considered a straight-line. Because the lane mark width in lane images is getting narrower as it is closer to the vanishing point and the LROI is established reflecting this condition, the shape of the LROI is like a triangular pyramid. Fig. 4 shows the establishment of the LROI in case of the left-curved lane, straight lane, and right-curved lane, respectively. In the figure, the solid lines represent the LCFs.

In LROI, the edges are extracted. Then, the phase angle of the extracted edge is compared with the computed slope of LCF for each pixel in the LROI. From this comparison, the LCF most identical to the lane boundary is found.

3.2. The comparison of the lane edge feature and the LCF feature

The LCF most identical to the lane boundary can be found by the comparison of the lane edge feature and the LCF feature. The edge features are composed of the magnitude $\nabla g(x_f, y_f)$, and the

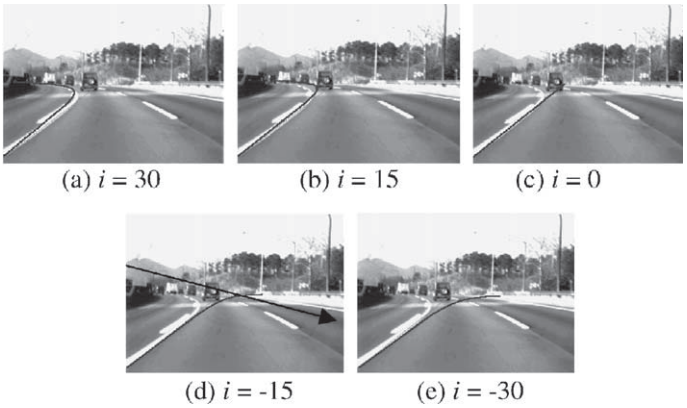

Fig. 3. LCFs for the various i in Eq. (10). The solid line is the LCF and the value of i is 30, 15, 0, −15, and −30, respectively.

Fig. 4. The establishment of the LROI. The triangular pyramid shape is the LROI. Left: left-curved lane. Middle: straight lane. Right: right-curved lane.

phase angle $\alpha(x_f, y_f)$. Their numerical expressions are as follows:

$$\nabla g(x_f, y_f) = \sqrt{G_{x_f}^2 + G_{y_f}^2} \approx |G_{x_f}| + |G_{y_f}| \tag{11}$$

$$\alpha(x_f, y_f) = \tan^{-1}\left(\frac{G_{y_f}}{G_{x_f}}\right) \tag{12}$$

where

$$[\, G_{x_f} \quad G_{y_f} \,] = \left[\frac{\partial g}{\partial x_f} \quad \frac{\partial g}{\partial y_f}\right]$$

The LCF feature is the slope of the LCF, y'_f, which is represented as follows:

$$y'_f(x_f) = a \pm \frac{2cx_f + d}{2\sqrt{cx_f^2 + dx_f + e}} \tag{13}$$

Then, the angle of y'_f is as follows:

$$\beta(x_f) = \tan^{-1}(y'_f(x_f)) \tag{14}$$

The similarity of the edge phase angle and the LCF slope angle is evaluated as follows:

$$D_j = \lfloor \alpha^j(x_f, y_f) - \beta^j(x_f) \rfloor, \quad j = 1, \ldots, N_i \tag{15}$$

where N_i is the number of pixels exceeding the threshold value of the magnitude of the edge pixels in the ith LROI, in which i was defined by Eq. (10).

To count the number of the cases that the similarity value of Eq. (15) exits at a certain range of $\pm\delta$, we construct a histogram such that

$$\text{if} \quad -\delta \leqslant D_j \leqslant \delta, \quad H_l = H_l + 1,$$
$$l \text{ is the integer value of } D_j \tag{16}$$

Here, all the initial values of H_l are zero for $1 \leqslant j \leqslant N_i$, and $l = -15, \ldots, 15$. j and l are integers. The value of δ in Eq. (16) is set as 15. Then, the comparison of the lane edge and the LCF is expressed as $\widetilde{V}_i$, which is calculated by the summation of the histogram H_l, and as follows:

$$\widetilde{V}_i = \sum_{l=-15}^{15} H_l \tag{17}$$

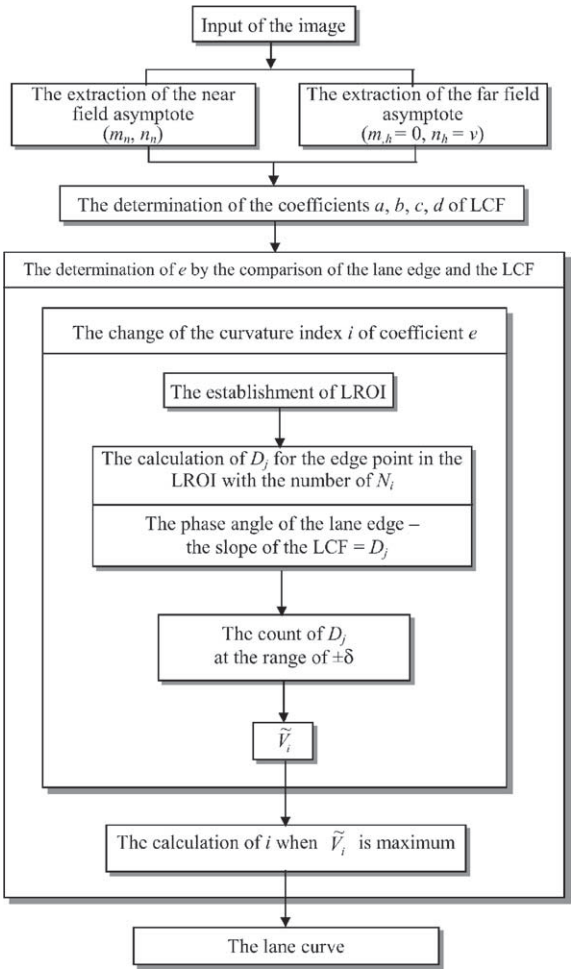

Fig. 5. The flow chart of the lane-curve detection.

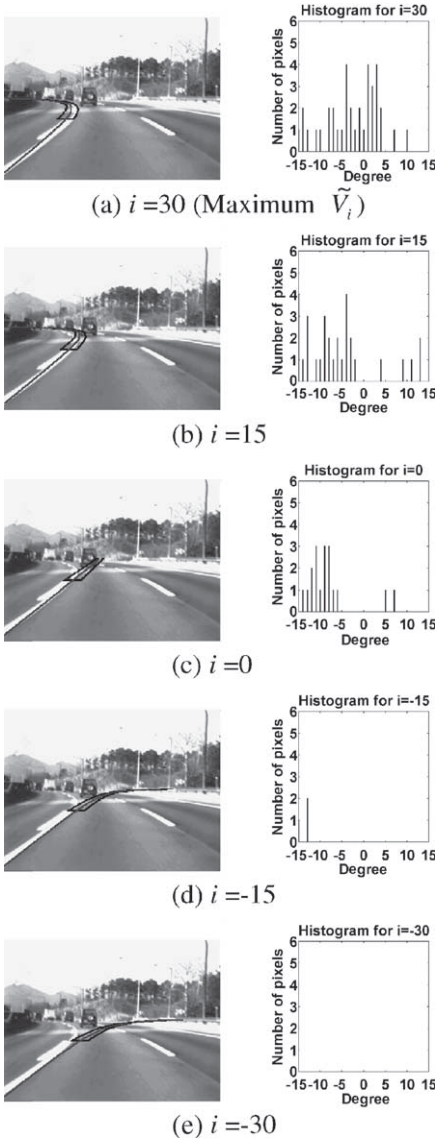

Fig. 6. The histogram of H_l: The value of i is 30, 15, 0, −15, and 30, respectively. The left images show the LROI, and the right graphs show the histogram of H_l. The area of the histogram is largest at $i = 30$.

In Eq. (17), the value i with the maximum value of $\widetilde{V}_i$ becomes the curvature index to be found. Fig. 5 shows the process of the proposed method, where the non-curvature-related coefficients of the LCF, a, b, c, d can be found by the near field asymptote and the far field asymptote, and the curvature-related coefficient of the LCF, e, can be found by the comparison of the lane edge and the LCF.

In Fig. 6, an example determining the curvature index i is shown, where only five cases for $i = 30$, 15, 0, −15 and −30 are shown with LCF and LROI. The right side graphs indicate the histogram of H_l obtained by Eq. (16). In this example, the direction of the lane-curve is left. Accordingly, we can guess the curvature a negative value and eventually the curvature index will be positive as we already explained in the previous section. As expected, the LCF constructed by the value $i = 30$ gives the largest $\widetilde{V}_i$ and shows the shape most identical to the real lane-curve.

4. Experimental results and discussions

The road for the experiment is the superhighway from Seoul to Cheongju, Korea. Among the various road sections, a suitable section was selected, which has left curves, right curves, and straight road sections. In the experiment, a CCD camera was equipped at the room mirror, and road images were recorded on a videotape. In the selected road section, 2000 images were captured continuously. The curve pattern of the captured images was successively straight, right turn, straight, left turn, straight, left turn, and straight. The curve pattern is shown in Fig. 7.

Fig. 8 shows the result of the lane-curve detection that is calculated by the proposed method. In the graph of the figure, the horizontal axis represents the frame number of the sequential images, and the vertical axis depicts the value of curvature index i obtained by Eq. (17). The negative value of the curvature index i in the graph indicates the right-curved lane, the positive value indicates the left-curved lane, and the value zero indicates the straight lane. In the transition section of the road direction, which changes from the right-curved lane into the straight lane and so on, the value of i increases or decreases gradually. Fig. 8 coincides well with the original curve pattern of Fig. 7, considering the converted sign of the curvature index i.

In Fig. 9, we show several cases among 2000 frames in Fig. 8. The images, which were troublesome for detecting the lane-curve, were selected

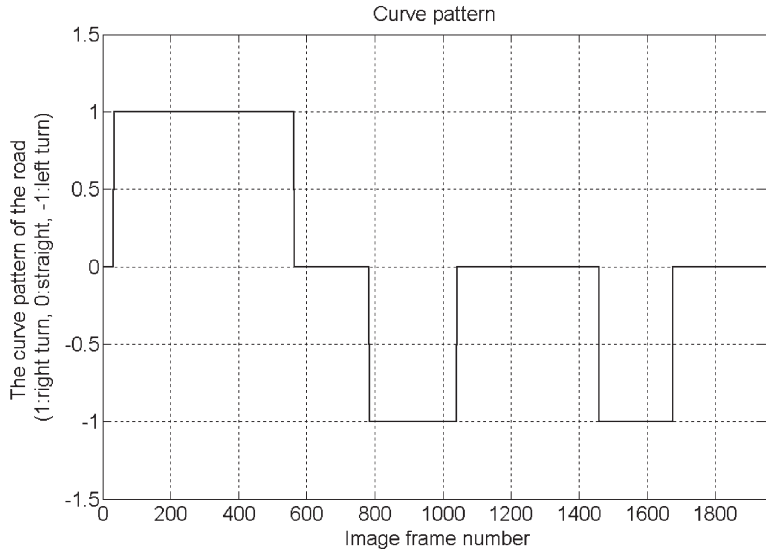

Fig. 7. The pattern of lane-curved direction. The x-axis indicates the frame number and the y-axis indicates the curve pattern; right-curved lane has 1, straight lane has 0, and left-curved lane has -1.

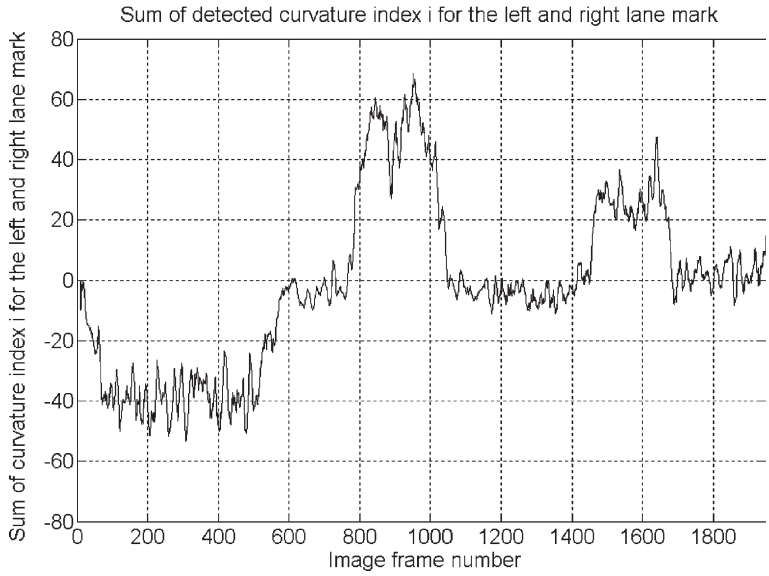

Fig. 8. The distribution of curvature index i. The x-axis indicates the image frame number, and the y-axis shows the summation result of the detected curvature index i for the left and right lane mark.

and enumerated in the order of the capturing sequence of the road images. The selected images have various noises such as the wear of road surface, the shadow and the occlusion of lane marks by other vehicles. However, the detected LCF coincides well with the lane-curve. Therefore, the lane detection is not affected by the local noise for the lane mark. The experimented road is

Fig. 9. The detected LCF in the road images. The solid lines indicate the detected LCFs. The result images were enumerated in the order of the capturing sequence of the road images.

the superhighway and has a continuous change of the vertical slope. But the maximum vertical slope of the superhighway is just 2%, so a slight uphill road and downhill road can be confirmed in Fig. 9.

Now, the applicability of the proposed method, including the novel LCF and the determination of the coefficients of the LCF, is evaluated by deriving the curvature of the lane-curve on the world coordinate using the detected value of i in Fig. 8. The curvature parameter A of Eq. (1) is derived from Eq. (8) as follows:

$$A = -\frac{kd_{px}d_{py}}{\lambda^2 T_z} \tag{18}$$

where λ is the focal length, T_z is the camera location from the ground, and d_{px} and d_{py} are the camera-related parameters. d_{px} and d_{py} are explained in Eq. (A.5) of Appendix A. The camera calibration was only performed to convert the curvature index i to the curvature parameter A of Eq. (18). The parameters obtained by the camera calibration are shown in Table 1.

In Fig. 10, the values of the curvature parameter A of Eq. (18) are shown, which were calculated from the values of i of Fig. 8. The lane curvature is positive in the right-curved lane and negative in the left-curved lane. Also, the lane curvature is zero in the straight lane. In the transition section of the road direction, the lane curvatures

Table 1
The camera parameters and the frame capturing parameters

Parameter	Value (mm)	Parameter	Value (number)
f	1.4002733×10	C_x	160
T_z	1.162784498×10^3	C_y	120
d_{px}	2.04375×10^{-2}	N_{cx}	768
d_{py}	2.0375×10^{-2}	N_{cy}	494
d_x	8.515625×10^{-3}	N_{fx}	320
d_y	9.898785×10^{-3}	N_{fy}	240

increase or decrease gradually, which is the same tendency as shown in Fig. 8.

The radius of the curvature is calculated through the reciprocal of the curvature A. The extracted radius of the curvature is approximately 1000 m in the section of curved lane, and the minimum value of the radius of curvature is 637 m. According to the specifications of superhighway construction of the Republic of Korea, the minimum of the radius of curvature is 460 m for the 100 km/h-speed-limit superhighway. The experiment road was a 100 km/h-speed-limit superhighway. Therefore, the extracted radius of curvature satisfies the superhighway construction specifications, and the conversion of the curvature index i to the lane curvature A is suitably performed.

In Fig. 10, a road section divided by Fig. 7 is shown. (a)–(d) of Fig. 10 indicate the divided road section, and are respectively the right-curved, first left-curved, second left-curved and straight road. The average and standard deviation of the detected curvature of each road section is shown in Table 2. The curvature is also divided into three intervals for the left-curved, straight and right-curved road in Table 2. To divide the curvature, the minimum and maximum value of the curvature for the curved road must be defined. The minimum value of the curvature for the curved road is 0.313×10^{-3} m^{-1}, which is the minimum absolute value of the detected curvature of the curved road section of Fig. 10. The maximum value of the curvature is 2.17×10^{-3} m^{-1}, which is the reciprocal of 460 m, the minimum of the radius of curvature. Therefore, the intervals for the left-curved, straight, and right-curved road are respectively, -2.17×10^{-3} to -0.313×10^{-3} m^{-1}, -0.313×10^{-3} to 0.313×10^{-3} m^{-1} and 0.313×10^{-3} to 2.17×10^{-3} m^{-1}. These three intervals are expressed as 'Defined interval' in Table 2. On the

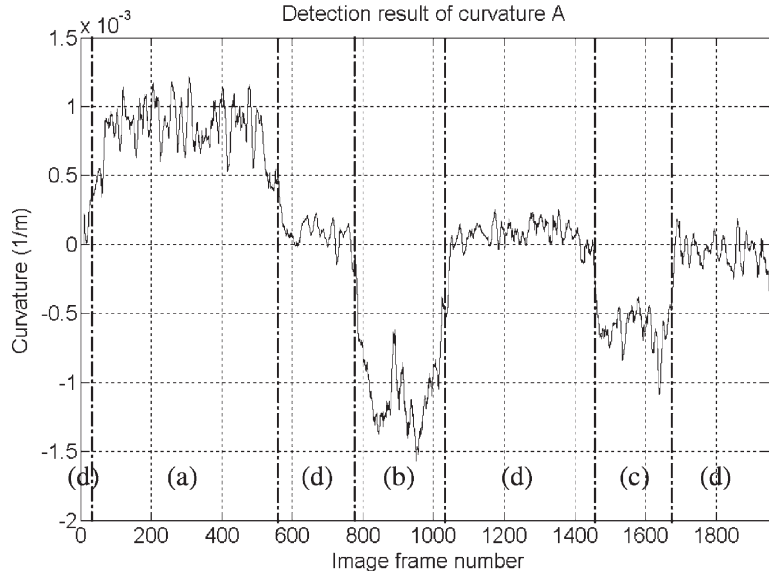

Fig. 10. The detection result of the curvature A. The x-axis indicates the image frame number and the y-axis indicates the detected curvature. (a)–(d) are the road sections divided by Fig. 7, and respectively the right-curved, first left-curved, second left-curved and straight road.

Table 2
The analysis of the curvature detection result of Fig. 10

Road section of Fig. 10	Average (m^{-1})	Standard deviation (m^{-1})	Defined interval (m^{-1})	Probability for defined interval (%)
Right-curved (a)	0.826×10^{-3}	0.199×10^{-3}	0.313×10^{-3} to 2.17×10^{-3}	99.51
First left-curved (b)	-1.036×10^{-3}	0.275×10^{-3}	-2.17×10^{-3} to -0.313×10^{-3}	99.57
Second left-curved (c)	-0.605×10^{-3}	0.136×10^{-3}	-2.17×10^{-3} to -0.313×10^{-3}	98.42
Straight (d)	0.039×10^{-3}	0.115×10^{-3}	-0.313×10^{-3} to 0.313×10^{-3}	98.99

assumption that the detected curvature has a normal distribution, the probability for the defined interval was calculated using the average and standard deviation of the detected curvature of each road section. The calculated probability for the defined interval is shown in Table 2. The probabilities for the road section (a)–(d) of Fig. 10 are respectively 99.51%, 99.57%, 98.42%, and 98.99%. Therefore, the recognition performance of the curve direction is good.

5. Conclusion

In this paper, a novel algorithm based on the LCF was proposed to detect the lane-curve on the road. The proposed algorithm showed excellence of the lane-curve detection in the application to lane images. While the many existing algorithms have depended on the top-view image generation based on camera calibration, the proposed algorithm needs no data relating between the lane and the camera during the lane detection process. The proposed algorithm assumes that the road surface is flat. However, the performance of the proposed algorithm did not deteriorate in uphill or downhill sections of the superhighway. But, the superhighway has just maximum 2% of vertical slope, so the proposed algorithm is only useful for the slight uphill and downhill road.

The proposed algorithm estimates the coefficients of the LCF with the precondition that the near field lane boundary and the vanishing point are detected. Therefore, the performance of the lane-curve detection relies on the accuracy of the near field and the far field asymptote. The far field asymptote can be found from the intersection between the near field asymptote for the left lane mark and the near field asymptote for the right lane mark. Therefore, the accuracy of the asymptote can be determined by the identity of the near field asymptote with the lane mark near the camera. To estimate the accuracy of the asymptote, the lane width can be calculated by the transformation of the near asymptote to the world coordinate systems. The calculated lane width also can be compared with the exact lane width of the road. If these asymptotes are accurate, the proposed algorithm can be applied to the superhighway as a simple and robust lane-curve detection method.

6. Summary

As the existing methods for the lane detection, there were the various types of the lane detection systems; the local-interest-region based, neural network based, and top-view-image generation based lane detection system. But, these systems have some defects respectively; the local detection error, neural network relearning for a new lane-form, and the top-view-image generation during the lane detection. To overcome these problems, in this paper, a new lane model in the image coordinate systems was developed and applied. The new lane model was obtained by the transformation of the defined parabolic function on the world coordinates into the image coordinates, which was named as the LCF. The LCF has the similar shape to the lane shape on the image, and all possible lane shapes on the image can be embodied by the change of parameters of the LCF. Therefore, to detect the lane, the value of each parameter to represent the LCF most identical to the lane must be found. For this, the analysis of the parameters of the LCF was performed, and they were classified into the curvature-related parameters and the non-curvature-related parameters. The non-curvature-related

parameters were found by the asymptote of the LCF, and then the curvature-related parameter was found by the substitution for a value proportional to the curvature in the range of the curvature limits of the superhighway. The proposed algorithm was experimented in the expressway section of the length about 4.5 km. The LCF most identical to the lane was detected and the curvature was calculated. As a result, the detected LCF accorded well with the lane shape, and the calculated curvature was valid.

Appendix A. Lane-curve function

The camera coordinates (x_c, y_c, z_c) are expressed by the world coordinates $(x, y, 0)$, the rotation matrix R and translation matrix T as follows:

$$\begin{bmatrix} x_c \\ y_c \\ z_c \end{bmatrix} = R\left[\begin{bmatrix} x \\ y \\ 0 \end{bmatrix} + T\right] = \begin{bmatrix} r_{xx} r_{xy} r_{xz} \\ r_{yx} r_{yy} r_{yz} \\ r_{zx} r_{zy} r_{zz} \end{bmatrix} \begin{bmatrix} x - T_x \\ y - T_y \\ -T_z \end{bmatrix} \tag{A.1}$$

If the pinhole camera model is assumed, the relationship between the image coordinates (x_i, y_i) and the camera coordinates is expressed as follows:

$$\begin{bmatrix} x_i \\ y_i \end{bmatrix} = \begin{bmatrix} \dfrac{\lambda x_c}{z_c} \\ \dfrac{\lambda y_c}{z_c} \end{bmatrix} = \begin{bmatrix} \lambda \dfrac{(x - T_x) r_{xx} + (y - T_y) r_{xy} - T_z r_{xz}}{(x - T_x) r_{zx} + (y - T_y) r_{zy} - T_z r_{zz}} \\ \lambda \dfrac{(x - T_x) r_{yx} + (y - T_y) r_{yy} - T_z r_{yz}}{(x - T_x) r_{zx} + (y - T_y) r_{zy} - T_z r_{zz}} \end{bmatrix} \tag{A.2}$$

where λ is focal length.

In the transformation from the world coordinates to the camera coordinates, the translation along z-axis and the rotation of the 90° about the x-axis only are considered. Then, Eq. (A.2) is simplified as

$$\begin{bmatrix} x_i \\ y_i \end{bmatrix} = \begin{bmatrix} \dfrac{\lambda x_c}{z_c} \\ \dfrac{\lambda y_c}{z_c} \end{bmatrix} = \begin{bmatrix} \lambda \dfrac{x}{y} \\ \lambda \dfrac{T_z}{y} \end{bmatrix} \tag{A.3}$$

From Eq. (A.3), the following equation is obtained.

$$x = \frac{x_i T_z}{y_i}, \qquad y = \frac{\lambda T_z}{y_i} \tag{A.4}$$

The ideal image coordinates (x_i, y_i) can be transformed to the computer image coordinates (x_f, y_f) by the following equation:

$$\begin{aligned} x_i &= (x_f - C_x) d_{px} \\ y_i &= (y_f - C_y) d_{py} \end{aligned} \tag{A.5}$$

(here, $d_{px} = d_x(N_{cx}/N_{fx})$, $d_{py} = d_y(N_{cy}/N_{fy})$)

x_i, y_i ideal image coordinates
x_f, y_f computer image coordinates
C_x, C_y the center of the computer frame memory
N_{cx}, N_{cy} the number of the sensor elements in the x and y direction
N_{fx}, N_{fy} the number of pixels in the horizontal and the vertical line as sampled by the computer
d_x, d_y the center to center distance between the adjacent sensor elements in x and y direction

As explained in Eq. (1), the lane boundary on the road can be approximated to a parabola. If Eqs. (A.4) and (A.5) substitute for Eq. (1) and are simplified, a new mathematical expression is obtained as follows:

$$y_f = a x_f + b \pm \sqrt{c x_f^2 + d x_f + e} \tag{A.6}$$

where

$$\begin{aligned} a &= \frac{T_z d_{px}}{2 C d_{py}} \\ b &= \frac{-T_z C_x d_{px} - B\lambda T_z + 2 C_y C d_{py}}{2 C d_{py}} \\ c &= \frac{T_z^2 d_{px}^2}{4 C^2 d_{py}^2} \\ d &= -\frac{C_x d_{px}^2 T_z^2 + B\lambda T_z^2 d_{px}}{2 C^2 d_{py}^2} \\ e &= \frac{d_{px}^2 T_z^2 C_x^2 + 2B\lambda T_z^2 d_{px} C_x + B^2 \lambda^2 T_z^2 - 2CA\lambda^2 T_z^2}{4 C^2 d_{py}^2} \\ &= (b - C_y)^2 + \left(-\frac{A\lambda^2 T_z}{d_{px} d_{py}} \right) a \end{aligned} \tag{A.7}$$

Eq. (A.6) shows the projection of the world coordinates lane model to the image coordinates lane model. In this paper, the mathematical expression of Eq. (A.6) is called by the LCF.

Appendix B. The asymptote of the LCF

If the asymptote of the LCF is defined by $y_a = mx_a + n$, m and n can be calculate by the following equations.

$$\begin{aligned} m &= \lim_{x_f \to \infty} y'_f(x_f) \\ n &= \lim_{x_f \to \infty} [y_f(x_f) - x_f y'_f(x_f)] \end{aligned} \tag{B.1}$$

Lastly, the asymptote of the LCF is as follows:

$$y_a = (a \pm \sqrt{c})x_a + \left(b \pm \frac{d}{2\sqrt{c}}\right) \tag{B.2}$$

Appendix C. The relationship between the LCF and the asymptote

From Eqs. (A.7) and (B.2), the parameters of the asymptote of the LCF are constructed as follows:

$$\begin{aligned} m &= a \pm \sqrt{c} = \frac{T_z d_{px}}{C d_{py}} \text{ or } 0 \\ n &= b \pm \frac{d}{2\sqrt{c}} = -\frac{C_x d_{px} T_z + B\lambda T_z}{C d_{py}} + C_y \text{ or } C_y \end{aligned} \tag{C.1}$$

References

Behringer, R., 1994. Road recognition from multifocal vision. In: Proc. Intelligent Vehicle'94. pp. 302–307.

Bertozzi, M., Broggi, A., 1998. GOLD: A parallel real-time stereo vision system for generic obstacle and lane detection. IEEE Trans. Image Process. 7 (1), 62–81.

Bimbo, A.D., Landi, L., Santini, S., 1993. Determination of road directions using feedback neural nets. Signal Process. 32, 147–160.

Crisman, J., Thorpe, C., 1993. SCARF: A color vision system that tracks roads and intersections. IEEE Trans. Rob. Autom. 9 (February), 49–58.

Dickmanns, E.D., Mysliwetz, B.D., 1992. Recursive 3-D road and relative ego-state recognition. IEEE Trans. PAMI 14 (2), 199–213.

Enkelmann, W., Struck, G., Geisler, J., 1995. ROMA: A system for model-based analysis of road markings. In: Masaky, I. (Ed.), Proc. IEEE Intelligent Vehicle'95 Conf., Detroit, MI. pp. 356–360.

Kluge, K., Thorpe, C., 1992. Representation and recovery of road geometry in YARF. In: Intelligent Vehicles'92 Symposium, Proc. IEEE. pp. 114–119.

Lee, J.W., Yi, U.K., Baek, K.R., 2001. A cumulative distribution function of edge direction for road-lane detection. IEICE Trans. Inf. Syst. E84-D (9), 1206–1216.

Park, J.W., Jhang, K.Y., Lee, J.W., 2001. Detection of lane curve direction by using image processing based on neural network and feature extraction. J. Imaging Sci. Technol. 45 (1), 69–75.

Pomerleau, D.A., 1994. Neural Network Perception for Mobile Robot Guidance. Kluwer Academic, Boston.

Pomerleau, D.A., 1995. RALPH: Rapidly adapting lateral position handler. In: Proc. Intelligent Vehicles'95 Symposium, Detroit, USA. pp. 506–511.

Risack, R., Mohler, N., Enkelmann, W., 2000. A video-based lane keeping assistant. In: Proc. IEEE Intelligent Vehicles Symposium 2000, Dearborn, MI, October 3–5. pp. 356–361.